

## Additional evidence for fusion-fission in $^{32}\text{S} + ^{24}\text{Mg}$ reactions: Division of excitation energy and spin in the fission fragments

S. J. Sanders

*Department of Physics and Astronomy, University of Kansas, Lawrence, Kansas 66045  
and Argonne National Laboratory, Argonne, Illinois 60439*

B. B. Back, R. V. F. Janssens, D. G. Kovar, D. Habs,\* D. Henderson, T.-L. Khoo,  
H. Korner,† G.-E. Rathke,† T. F. Wang,‡ and F. L. H. Wolfs  
*Argonne National Laboratory, Argonne, Illinois 60439*

K. B. Beard

*Department of Physics, University of Notre Dame, South Bend, Indiana 46556  
(Received 27 November 1989)*

We have measured  $\gamma$  rays in coincidence with  $^{12}\text{C}$  fragments from the fission of  $^{56}\text{Ni}$  produced with the  $^{32}\text{S} + ^{24}\text{Mg}$  reaction at  $E_{\text{lab}} = 140$  MeV. These data provide insight into the fission process in this light system by giving information about the energy and spin sharing between the  $^{12}\text{C}$  and  $^{44}\text{Ti}$  fragments, and the spin alignment of the lighter,  $^{12}\text{C}$  fragment. The spin transfer and the nuclear "temperature" at scission deduced from this measurement can be related to the compound-nucleus spin and potential energy at scission. The results indicate a statistical decay process consistent with the predictions of the transition-state model employing newer estimates of the spin- and mass-asymmetry-dependent saddle-point energies and corresponding shapes. No evidence is found for the spin alignment of the  $^{12}\text{C}$  fragments, contrary to what might be expected for a deep-inelastic scattering origin of the fully energy damped yields.

The transition-state model for nuclear fission has been shown to successfully describe the magnitude and mass dependence of the fully energy damped, binary reaction products from heavy-ion reactions leading to compound nuclei as light as  $^{56}\text{Ni}$ .<sup>1</sup> The primary difference in its application in light systems, as compared to heavier systems, is the need to incorporate the spin- and mass-asymmetry-dependent saddle-point energies for the compound system in order to establish the transition-state phase space.<sup>2</sup> The application of the ideas of nuclear fission in such light systems is not without controversy, however, since the saddle-point phase space used to describe the fission process is very similar to that appropriate for a dinuclear, orbiting complex, suggesting the possibility of a deep-inelastic scattering process.<sup>3,4</sup> In this paper we study the energy sharing between fragments from the asymmetric breakup of the  $^{56}\text{Ni}$  system. This system was produced with the  $^{32}\text{S} + ^{24}\text{Mg}$  reaction at  $E_{\text{lab}}(^{32}\text{S}) = 140$  MeV; close to the beam energy employed in our earlier particle-particle coincidence measurement.<sup>1,5</sup> We have measured  $\gamma$  rays in coincidence with  $^{12}\text{C}$  fission fragments. From these data, the relative population of the  $^{12}\text{C}$  ( $4.44$  MeV;  $J^\pi = 2^+$ ) state and the  $^{12}\text{C}$  ground state is found to indicate a strong thermalization of the  $^{12}\text{C}$  reaction products. The temperature deduced for the decaying complex is close to that expected for the compound-nucleus saddle point. (In light nuclei, the saddle and scission points are thought to be similar.<sup>6</sup>) In addition, no evidence is found for the spin alignment of the  $^{12}\text{C}$  fragments, again suggesting a statistical mechanism for the  $^{12}\text{C}$  production.

Particle- $\gamma$  coincidences were measured using a pulsed beam of 140 MeV  $^{32}\text{S}$  incident on a  $150 \mu\text{g}/\text{cm}^2$   $^{24}\text{Mg}$  target. The  $\gamma$  rays were detected with the Argonne-Notre-

Dame  $\gamma$ -ray facility,<sup>7</sup> with the forward-angle  $\gamma$ -ray detectors ( $\theta_{\text{lab}} < 60^\circ$ ) removed to accommodate particle detectors. This left eight Ge detectors and a 42 element BGO array surrounding the target. The energy calibrations and relative efficiencies of the Ge detectors were determined using standard  $\gamma$ -ray sources.

The  $^{12}\text{C}$  fission fragments were detected using 25 separate Si detectors covering a total solid angle of  $\sim 60$  msr, located at angles with  $8^\circ \leq \theta \leq 45^\circ$ . The masses of the reaction products were obtained from the measured energies and flight times. Unit mass resolution was achieved up to mass  $A = 32$  for all of the detectors, and to mass  $A = 48$  for the detectors located at  $\theta \leq 12^\circ$ .

Both particle singles and particle- $\gamma$  coincidence data were collected. The particle- $\gamma$  event trigger required a triple coincidence among a particle detector, at least one of the BGO detectors, and at least one Ge detector. (The experimental bias resulting from the triple coincidence requirement will be discussed below.)

Previous measurements<sup>1,5</sup> have shown that the  $^{12}\text{C}$  fragments produced in the  $^{32}\text{S} + ^{24}\text{Mg}$  reaction at  $E_{\text{lab}}(^{32}\text{S}) = 140$  MeV are fully energy damped and result from a binary process. Only a small number of the observed  $^{12}\text{C}$  fragments arise from  $\alpha$ -particle decay of heavier mass fragments. Although the earlier data do not preclude the possibility of mass  $A = 13$  production, which can form  $^{12}\text{C}$  after single nucleon emission, this is deemed unlikely by the observed systematics of the fission process in  $^{56}\text{Ni}$  which is found to favor those channels with the greater ground-state binding energies.

The relative amount of energy in the  $^{12}\text{C}$  and  $^{44}\text{Ti}$  fragments can be deduced from the measured reaction  $Q$  value and the relative population of the  $^{12}\text{C}$  ground state and

4.44 MeV, first-excited state. The  $\gamma$  rays detected in the germanium detectors were Doppler corrected and sorted into efficiency-corrected spectra according to either the velocity of the  $^{12}\text{C}$  particle or the corresponding  $^{44}\text{Ti}$  recoil velocity, as shown in Figs. 1(a) and 1(b), respectively. As expected, the spectrum corrected for the  $^{12}\text{C}$  fragment velocity shows a Doppler broadened peak at 4.44 MeV ( $2^+ \rightarrow 0^+$  transition in  $^{12}\text{C}$ ). The recoil-corrected spectrum [Fig. 1(b)] shows a number of lines which can be identified as transitions in residues from the  $^{44}\text{Ti}$  recoil:  $^{36}\text{Ar}$ ,  $^{38}\text{Ar}$ ,  $^{39}\text{K}$ ,  $^{40}\text{Ca}$ ,  $^{42}\text{Ca}$ ,  $^{42}\text{Sc}$ , and  $^{43}\text{Sc}$ . No evidence is found for  $\gamma$  rays arising from the  $^{44}\text{Ti}$  nucleus itself.

The total  $^{12}\text{C}$  production rate  $Y_{\text{tot}}$  can be obtained from the sum of the measured yields of the ground-state transitions of the various  $^{44}\text{Ti}$  residues. (The population of high-spin isomeric states in  $^{42}\text{Ca}$  and  $^{43}\text{Sc}$  was considered by observing the transitions populating these states.) Together with the observed population of the  $^{12}\text{C}$  (4.44 MeV;  $2^+$ ) excited state  $Y_{2^+}$ , the relative population of the  $^{12}\text{C}$  excited state and ground state can be established, with the ratio  $R(2^+/\text{g.s.}) = Y_{2^+} / (Y_{\text{tot}} - Y_{2^+})$ , where  $\alpha$  is the ratio of the population of higher-lying  $^{12}\text{C}$  states to the  $^{12}\text{C}$  ground state. This expression, an approximation valid for small values of  $\alpha$ , is obtained by noting that all of the higher-lying states with significant statistical population decay primarily by particle emission, and have only weak  $\gamma$ -ray branches. The deduced population ratio does not depend on the geometry of the particle detectors.

To correct our results for low  $\gamma$ -ray multiplicity events, where the gating requirement of two detected  $\gamma$  rays might not be satisfied, a Monte Carlo simulation of the BGO multiplicity response was used in conjunction with statistical evaporation calculations using the code CASCADE (Ref. 8) to estimate the missing yield from the

population of low-lying states. For the CASCADE calculation the  $^{44}\text{Ti}$  excitation energy was taken directly from the measured reaction  $Q$  value, assuming population of either the ground or first-excited states of  $^{12}\text{C}$ . The average  $^{44}\text{Ti}$  spin was deduced from a model of the fission decay process. Based on the analysis of Ref. 1, a  $^{56}\text{Ni}$  spin of  $J = 36\hbar$  was assumed which, in the sticking limit for the asymmetric saddle-point shape appropriate for  $^{12}\text{C} + ^{44}\text{Ti}$  fission, results in  $11\hbar$  of spin being transferred to the fragments. A Gaussian distribution was assumed for the total spin transferred to the fragments with a mean of  $11\hbar$  and a variance of  $2\hbar$ . The  $^{12}\text{C}$  fragments receive either  $0\hbar$  or  $2\hbar$  units.

The results of the CASCADE calculation are compared to the experimental results in Figs. 2 and 3, respectively. The observed  $\gamma$ -ray transitions for the  $^{44}\text{Ti}$  residues are indicated in Fig. 2; the level schemes are from Refs. 9-12. The solid and dashed lines indicate the populations predicted for the  $^{12}\text{C}$  fragment being formed in its ground state and first-excited state, respectively (fitting the predicted distributions with Gaussian shapes). It is seen that the population of the heavier residues ( $^{40}\text{Ca}$ ,  $^{42}\text{Ca}$ ,  $^{42}\text{Sc}$ , and  $^{43}\text{Sc}$ ) is expected to occur at a sufficiently high excitation energy that a cascade of several  $\gamma$  rays would be expected, leading to a high probability of generating a good event trigger. The three lighter residues ( $^{36}\text{Ar}$ ,  $^{38}\text{Ar}$ , and  $^{39}\text{K}$ ) are found, however, to have appreciable population of the low-lying levels, necessitating a correction for the trigger bias. Histograms indicating the fraction of the total  $^{44}\text{Ti}$  fragment yields leading to specific final residues are shown in Fig. 3. The partially cross-hatched histograms with uncertainties indicated are the experimental results. The observed yield is represented by the cross-hatched portion of these histograms and the correction to these yields based on the CASCADE calculation, and the BGO response simulation is given by the open part. The

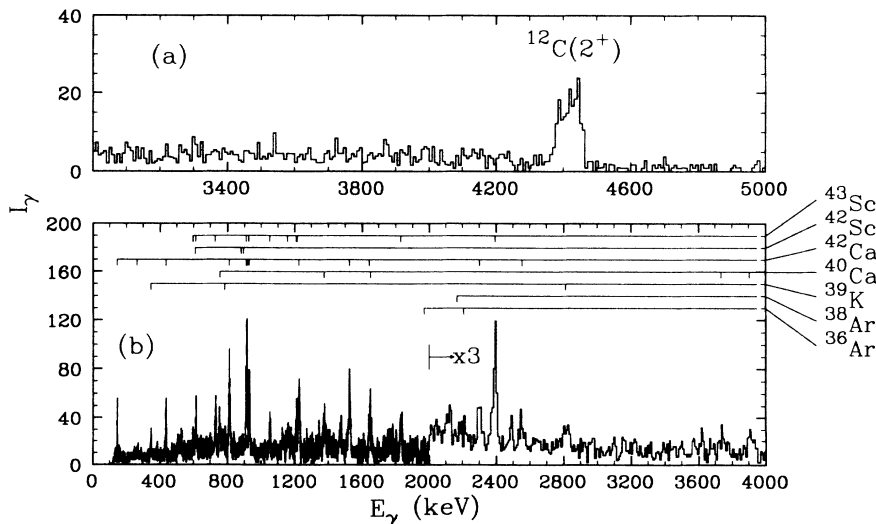


FIG. 1.  $\gamma$ -ray spectra measured in coincidence with  $^{12}\text{C}$  fragments. The spectra have been corrected for detector efficiencies as well as for the Doppler shift. The latter correction was performed for both the velocities of (a) the  $^{12}\text{C}$  particles and (b) the complementary  $^{44}\text{Ti}$  fragments. Transitions which have been identified as belonging to specific final residues from  $^{44}\text{Ti}$  particle decay are indicated. The spectra are binned 8 keV/channel, except for energies below 2000 keV in the recoil corrected spectrum, which are binned 1 keV/channel.

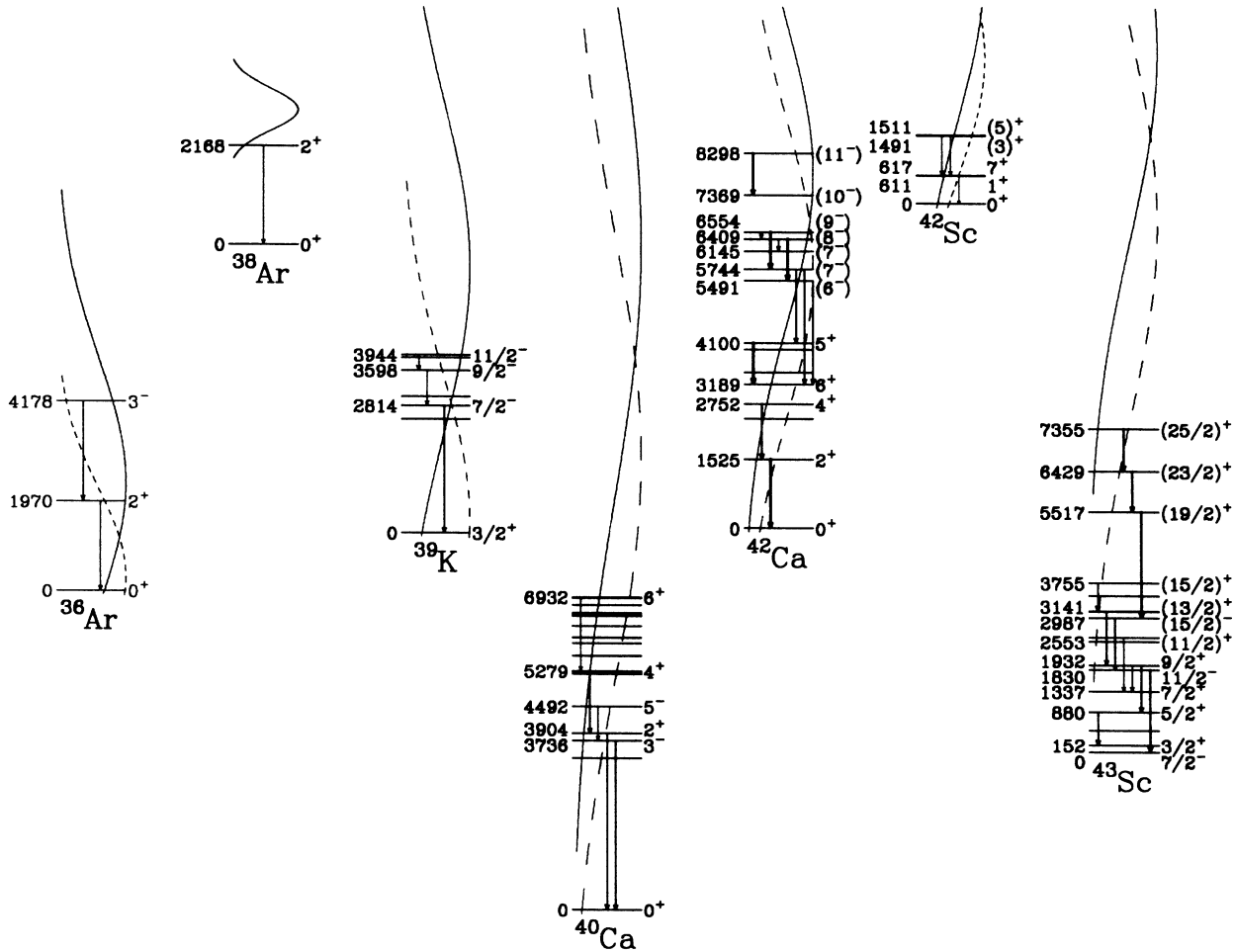


FIG. 2. Level diagrams for the  $^{44}\text{Ti}$  residues. The observed  $\gamma$ -ray transitions are indicated. Lines are drawn to indicate the low-lying states known to be populated through heavy-ion reactions in the various residues, although only those levels participating in observed transitions are labeled by their energies and spins. The Gaussian curves drawn through the level schemes indicate the CASCADE predicted population patterns for the residues, depending on whether the corresponding  $^{12}\text{C}$  particle is formed in its ground state (solid curves) or first-excited state (dashed curves). The level diagrams are offset by the ground-state binding energies of the respective fragments.

$^{12}\text{C}(2^+)$   $\gamma$ -ray yield was similarly corrected for the gating efficiency, as shown in Fig. 3 where the observed and corrected  $^{12}\text{C}(2^+)$  yields are indicated as fractions of the total  $^{44}\text{Ti}$  residue yield.

With these corrected yields we find the  $^{12}\text{C}$  population ratio  $R(2^+/\text{g.s.}) = 0.41 \pm 0.15(1+a)$ . The solid-open histograms in Fig. 3 are the results of the CASCADE calculations assuming this ratio. The fractional yields resulting from the  $^{12}\text{C}$  being in its ground and first-excited states are indicated by the solid and open parts of the histograms, respectively. Since the assumed relative population of  $^{12}\text{C}$  states affects the efficiency correction applied to the experimental results, an iterative procedure was followed to obtain this ratio. The efficiency correction factor, however, is not strongly dependent on the ratio assumed for the CASCADE calculations.

The dependence of the population ratio  $R$  on the average spin assumed transferred to the fragments (taken above as  $11\hbar$ ) was explored by repeating the calculations for different values of this spin. Changing this spin value affects the predicted final residue populations and, conse-

quently, the gating efficiency correction factor used in determining  $R$ . The inset in Fig. 3 shows the  $\chi^2/\text{degree-of-freedom}$  goodness-of-fit value obtained in comparing the calculated residue fractions to the gating-efficiency-corrected experimental values. The minimum of  $\chi^2$  is found for a total fragment spin near  $11\hbar$ , supporting our earlier choice of this value based on the transition-state model. The population ratio  $R$  is also shown and is found to depend only weakly on the assumed total fragment spin.

The measured population ratio can be converted into an effective nuclear "temperature" using the expression  $R(\text{excited state}/\text{g.s.}) = [(2s_{\text{ex}} + 1)/(2s_{\text{g.s.}} + 1)] \exp(-\Delta/\tau)$ , where  $s_{\text{ex}}$  and  $s_{\text{g.s.}}$  are the spins of the excited state and ground state, respectively,  $\Delta$  is the energy difference between the two states, and  $\tau$  is the effective nuclear "temperature."<sup>13</sup> In the  $^{12}\text{C}(4.44 \text{ MeV}; 2^+)$  case, the statistical factor in brackets  $[\ ] = 5$ , assuming a nonaligned configuration, and the energy difference  $\Delta = 4.44 \text{ MeV}$ . This expression is also used to estimate the contribution from higher-lying states, needed to determine the factor

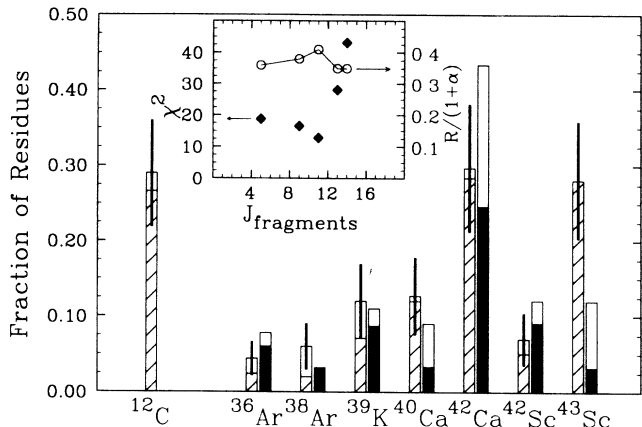


FIG. 3. Population of the  $^{12}\text{C}(2^+)$  state and the  $^{44}\text{Ti}$  residues expressed as fractions of the total residue yield. The partially cross-hatched histograms with uncertainties indicated are the experimental results, with the cross-hatched portions indicating the observed yields and the open portions showing the gating efficiency correction, as discussed in the text. The CASCADE predictions for the fragment populations are indicated by the solid-open histograms. Here the solid (open) portion corresponds to the  $^{12}\text{C}$  fragment being formed in its  $0^+$  ( $2^+$ ) state. The inset shows the  $\chi^2/\text{degree-of-freedom}$  goodness-of-fit value and the corresponding population ratio for different assumptions of the total spin transferred to the  $^{12}\text{C}$  and  $^{44}\text{Ti}$  fragments.

$(1 + \alpha)$ . We find, then,  $\tau = 1.8 \pm 0.3$  MeV with  $\alpha \sim 0.08$  (employing an iterative procedure and using the tabulation of Ref. 14 for the energies and spin values of  $^{12}\text{C}$  states up to 20 MeV excitation energy to determine  $\alpha$  for a given value of  $\tau$ ).

It is interesting to compare the “temperature” deduced from the relative state population with that used in determining the level density at the nuclear saddle point. In Ref. 1 it was shown that the fission mass distribution for  $^{56}\text{Ni}$  can be understood, quantitatively, based on the available phase space above the saddle-point energy. For the  $^{32}\text{S} + ^{24}\text{Mg}$  reaction at  $E_{\text{lab}}(^{32}\text{S}) = 140$  MeV, leading to  $^{12}\text{C} + ^{44}\text{Ti}$  fragments, a saddle-point energy of  $V_{\text{saddle}}(J = 36\hbar) \approx 46$  MeV was found. From this we can determine the level-density temperature by  $\tau_{\text{LD}} = [(E^* - V_{\text{saddle}})/a]^{1/2}$ , where  $E^*$  is the excitation energy of the  $^{56}\text{Ni}$  compound system and  $a$  is the level-density parameter. With  $E^* = 74$  MeV and  $a = 56/9.3$  (the level-density parameter found appropriate in the earlier analysis of Ref. 1 for the saddle point), we find  $\tau_{\text{LD}} = 2.2$  MeV, in reasonable agreement with the temperature deduced from the relative population of states in  $^{12}\text{C}$  considering the uncertainties in the two analyses. As a consistency check, the level-density temperature of the  $^{44}\text{Ti}$  recoil can be calculated from the excitation energy and spin found in this residue as deduced above, with  $\tau_{\text{LD}} = [(E^* - E_{\text{rot}})/a]^{1/2}$ , where  $E_{\text{rot}}$  is the rotational energy. Taking a weighted average for the  $^{44}\text{Ti}$  excitation energy and assuming that the  $^{12}\text{C}$  fragments are populated in the ground or first-excited states, respectively, one finds  $E^*(^{44}\text{Ti}) \approx 28.7$  MeV. The rotational energy can be determined using the results of Sierk<sup>15</sup> and has a weighted value of  $E_{\text{rot}} \approx 5.8$  MeV. Then using the level-density parameter  $a = \frac{44}{8}$  (as

employed in the CASCADE calculation for light-particle evaporation), we find  $\tau_{\text{LD}} = 2.0$  MeV, in agreement with the temperature obtained from the  $^{12}\text{C}$  state population.

The alignment of the  $^{12}\text{C}$  spin vector with respect to the normal to the reaction plane was determined by using the BGO array. The  $\gamma$ -ray energy spectra for the BGO detectors were Doppler corrected for the  $^{12}\text{C}$  velocity and sorted according to the efficiency weighted angle between the BGO detector and the normal to the reaction plane (defined by the  $^{12}\text{C}$  recoil direction and the beam direction). These distributions were normalized by the relative probability of observing a coincidence in each particle- $\gamma$  detector pair assuming isotropic emission of the  $\gamma$  rays in the  $^{12}\text{C}$  center-of-mass system.

The BGO spectrum in coincidence with  $^{12}\text{C}$  particles, summed over all angles, is shown as an inset in Fig. 4. The enhanced yield above the smooth, exponential background can be attributed to the full energy and escape peaks for the 4.44 MeV  $\gamma$  rays. The angular distribution for the  $^{12}\text{C}$  (4.44 MeV)  $\gamma$  rays with respect to the  $^{12}\text{C}$  reaction plane normal, expressed in the  $^{12}\text{C}$  center-of-mass system, is shown in Fig. 4. The data have been sorted into four equal-sized angular ranges between  $0^\circ$  and  $90^\circ$  using the symmetry of the radiation pattern about the reaction plane to combine the data with  $\theta_\gamma > 90^\circ$  with those for  $\theta_\gamma < 90^\circ$ . Since many detector combinations are combined for each data point, these points have been positioned at the yield and efficiency weighted angles. The range of angles covered are indicated by the horizontal

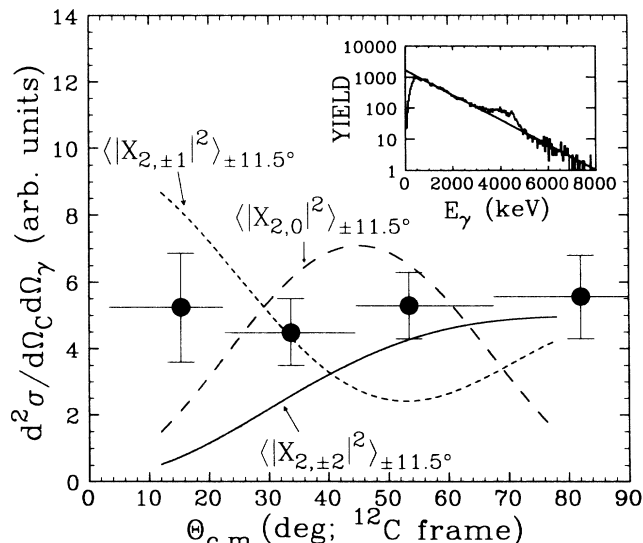


FIG. 4. Angular correlation of the  $^{12}\text{C}$  (4.44 MeV,  $2^+$ )  $\gamma$  rays with respect to the normal to the reaction plane. The vector spherical harmonics indicating the predicted radiation patterns for specific magnetic substates are indicated. These patterns have been angle averaged over  $\pm 11.25^\circ$ , comparable to the angle averaging of the experimental results. The inset shows the Doppler corrected, BGO detector  $\gamma$ -ray energy spectrum obtained by summing all particle- $\gamma_{\text{BGO}}$  coincidences for the 25 Si detectors and the 42 BGO detectors. The line through the data indicates an exponential background fit. The peak above this background corresponds to the full energy and single-escape peaks for the  $^{12}\text{C}(2^+ \rightarrow 0^+)$  transition.

lines. No evidence for alignment of the  $^{12}\text{C}$  fragment with respect to the reaction plane is observed. The experimental uncertainties largely reflect the uncertainty in the background subtraction of the BGO spectra. The curves in Fig. 4 show the polar-angle dependence of the quadrupole radiation pattern  $^{16} |X_{2m}|^2$  for different values of the magnetic quantum number  $m$ . These patterns have been angle averaged over  $\pm 11.25^\circ$ , comparable to the angle averaging of the experimental results. Full spin alignment normal to the reaction plane would have  $m = \pm 2$ .

Any alignment which may be present is small. Other measurements of spin alignment for quasielastic and partially energy damped deep-inelastic scattering fragments in lighter systems have found quite large spin alignments.<sup>17-19</sup> The absence of spin alignment in the present measurement suggests that a greater degree of statistical equilibration may be obtained in the asymmetric fission of  $^{56}\text{Ni}$  formed in the  $^{32}\text{S} + ^{24}\text{Mg}$  reaction than found in these earlier measurements where the entrance- and exit-channel mass asymmetries were more similar.

In summary, we have measured particle- $\gamma$  coincidences for the mass-identified fragments from  $^{56}\text{Ni}$  decay as populated with the  $^{32}\text{S} + ^{24}\text{Mg}$  reaction at  $E_{\text{lab}}(^{16}\text{O}) = 140$  MeV. The data for the  $^{12}\text{C} + ^{44}\text{Ti}$  fission channel have been analyzed to determine the distribution of energy and spin, and the degree of spin alignment of the  $^{12}\text{C}$  frag-

ment. The relative amount of energy found in the  $^{12}\text{C}$  and  $^{44}\text{Ti}$  fragments suggests that the  $^{12}\text{C}$  fragment is emitted statistically from a thermal source, the temperature of which is consistent with that predicted for the saddle-point configuration of the  $^{56}\text{Ni}$  compound system. The total spin transferred to the two fragments is found to be in agreement with the predicted spin transferred based on the expected saddle-point shape. There is no evidence that the  $^{12}\text{C}$  fragment is emitted in a spin-aligned configuration. The absence of an aligned component in  $^{12}\text{C}$  fragments indicates a high degree of statistical equilibration in this asymmetric mass channel from the  $^{32}\text{S} + ^{24}\text{Mg}$  reaction. These results, together with earlier measurements of the mass dependence of the fully energy damped yields in this system, all indicate a high degree of statistical equilibration in the compound system, and are contrary to what would be expected from a deep-inelastic scattering mechanism. The techniques developed in this measurement should be useful in the further scrutiny of the newer macroscopic energy calculations<sup>15</sup> that include effects resulting from the finite range of the nuclear interaction and the diffuseness of nuclear surfaces.

This work was supported by the U.S. Department of Energy, Nuclear Physics Division, under Contracts No. DE-FG02-89ER40506 and No. W-31-109-ENG-38.

\*Present address: Max-Planck-Institut, Heidelberg, Federal Republic of Germany.

†Present address: Technische University, Munich, Federal Republic of Germany.

‡Present address: Lawrence Livermore National Laboratory, Livermore, CA 94550.

<sup>1</sup>S. J. Sanders, D. G. Kovar, B. B. Back, C. Beck, D. J. Henderson, R. V. F. Janssens, T. F. Wang, and B. D. Wilkins, *Phys. Rev. C* **40**, 2091 (1989).

<sup>2</sup>L. G. Moretto, *Nucl. Phys.* **A247**, 211 (1975).

<sup>3</sup>D. Shapira, *Phys. Rev. Lett.* **61**, 2153 (1988).

<sup>4</sup>W. Dünneberger, A. Glaesner, W. Hering, D. Konnerth, R. Ritza, W. Trombik, J. Czakański, and W. Zipper, *Phys. Rev. Lett.* **61**, 927 (1988).

<sup>5</sup>S. J. Sanders, D. G. Kovar, B. B. Back, C. Beck, B. K. Dichter, D. Henderson, R. V. F. Janssens, J. G. Keller, S. Kaufman, T.-F. Wang, B. Wilkins, and F. Videback, *Phys. Rev. Lett.* **61**, 2154 (1988).

<sup>6</sup>K. T. R. Davies, R. A. Managan, J. R. Nix, and A. J. Sierk, *Phys. Rev. C* **16**, 1890 (1977).

<sup>7</sup>R. V. F. Janssens, T. L. Khoo, E. Funk, U. Garg, J. Kolata, and J. Mihelich, in *A Proposal for a BGO Sum-Energy/Multiplicity Spectrometer and a Multi-Compton Suppression Spectrometer System* (unpublished).

<sup>8</sup>F. Pühlhofer, *Nucl. Phys.* **A280**, 267 (1977).

<sup>9</sup>P. M. Endt and C. Van der Leun, *Nucl. Phys.* **A310**, 1 (1978).

<sup>10</sup>H. M. Sheppard, P. A. Butler, R. Daniel, P. J. Nolan, N. R. F. Rammo, and J. F. Sharpey-Schafer, *J. Phys. G* **6**, 511 (1980).

<sup>11</sup>A. R. Poletti, E. K. Warburton, J. W. Olness, J. J. Kolata, and Ph. Gorodetzky, *Phys. Rev. C* **13**, 1180 (1976).

<sup>12</sup>E. K. Warburton, J. J. Kolata, and J. W. Olness, *Phys. Rev. C* **11**, 700 (1975).

<sup>13</sup>D. J. Morrissey, W. Benenson, E. Kashy, B. Sherrill, A. D. Panagioutou, R. A. Blue, R. M. Ronningen, J. van der Plicht, and H. Utsunomiya, *Phys. Lett.* **148B**, 423 (1984).

<sup>14</sup>F. Ajzenberg-Selove, *Nucl. Phys.* **A433**, 1 (1985).

<sup>15</sup>A. J. Sierk, *Phys. Rev. C* **33**, 2039 (1986).

<sup>16</sup>J. D. Jackson, *Classical Electrodynamics* (Wiley, New York, 1962), p. 550.

<sup>17</sup>K. van Bibber, R. Ledoux, S. G. Steadman, F. Videbaek, G. Young, and C. Flaum, *Phys. Rev. Lett.* **38**, 334 (1977).

<sup>18</sup>A. Ray, D. D. Leach, R. Vandenbosch, K. T. Lesko, and D. Shapira, *Phys. Rev. Lett.* **57**, 815 (1986).

<sup>19</sup>G. Viesti, B. Fornal, F. Gramegna, G. Prete, R. A. Ricci, G. D'Erasmus, L. Fiore, G. Guarino, A. Pantaleo, I. Iori, A. Moroni, P. Blasi, and F. Lucarelli, *Z. Phys. A* **324**, 161 (1986).